LPV lateral control for ADAS based on driver performance monitoring

Ariel Medero, Olivier Sename, Vicenç Puig

LPV lateral control for ADAS based on driver performance monitoring ⋆

Ariel Medero [*,**] **Olivier Sename** [*] **Vicenç Puig** [**]

[*] *Univ. Grenoble Alpes, CNRS, Grenoble INP, GIPSA-Lab, 38000 Grenoble, France (e-mail: ariel.medero@grenoble-inp.fr, olivier.sename@grenoble-inp.fr).*
[**] *Institut de Robòtica i Informàtica Industrial (CSIC-UPC), C/. Llorens i Artigas 4-6, 08028 Barcelona, Spain (e-mail: ariel.medero@upc.edu, vicenc.puig@upc.edu).*

Abstract: This paper presents a lateral control Advanced Driver Assistance System for cars, which uses both steering control and differential braking commands to aid drivers and enhance vehicle safety. The proposed strategy uses a LPV PI Observer for the estimation of driver performance over a range of vehicle speeds. This estimation is then used as scheduling signals to activate / deactivate the ADAS actuators. The strategy is tested in simulation with randomly generated driver profiles to prove the adaptability to a diverse range of driver's behavior.

Keywords: Reconfigurable control, Linear parameter-varying systems, Intelligent driver aids.

1. INTRODUCTION

In this work we propose a Linear Parameter Varying (LPV) Lateral ADAS control which is activated based on driver's ability. The proposed strategy uses combined steering and differential braking as control actions. The estimation of driver's performance is obtained from an LPV PI Observer and some idealistic nominal driver models, which serves as the desired driver behaviour. From this estimation, scheduling functions are defined that modify the allowed control authority of the LPV ADAS Controller. The objective is here to use differential braking when driver errors are detected, and use the steering command only when this error become larger (while still minimizing the intrusiveness felt by the driver).

Some studies have designed lateral controllers considering the driver's lateral steering action through Driver Models. Let us mention some, e.g Gáspár et al. (2012); Khosravani et al. (2014); Chen et al. (2019). In these works the emphasis has been put on enhancing the ADAS controller robustness to variable human delay and parameter uncertainties to account for different levels of driving performances, as well as to other issues such as non linearities in the vehicle dynamics. However a limiting factor in all these strategies is that the ADAS controller is always active, which may be not desirable, see Mars et al. (2014). One prominent field in the vehicle lateral control problem with human drivers in the loop is the shared control proposition. Let us mention some recent works in shared control, e.g. Saleh et al. (2013); Erlien et al. (2015); Ji et al. (2018), where the main control approach is the optimal control theory, in order to solve some Model Predictive Control or $LQ/\mathcal{H}_2$ problems. However, in shared control it is assumed that the allocation of automation control authority can take a large percentage, which again, may not be desirable and feel invasive by the driver and trigger some users to disengage such systems.

The use of LPV PI Observers is widely covered in the literature for the problem of fault detection in sensors and actuators of non linear systems. Let us mention some recent works, e.g Youssef et al. (2017); Guzman et al. (2021). In our study, the driver performance estimation problem is recast as an additive fault estimation on the output of the nominal driver system, which is similar to the case of an additive sensor fault. The synthesis of the LPV/$\mathcal{H}_\infty$ PI Observer is here carried out using a Parameter Dependent Lyapunov Function, from the dual approach used for the synthesis of the LPV State-Feedback ADAS controller.

A preliminary study has been presented in Medero et al. (2021), concerning the case in which the driver error detection is carried out using the Parity Space approach with the assumption of an LTI driver model and constant longitudinal speed of the vehicle, with the steering wheel as the only actuator considered for the lateral ADAS controller. The main contributions of this paper are first to extend the driver error detection method to the case of a varying vehicle speed (using an LPV PI Observer), and to develop a control algorithm, considering not only the steering angle but also the differential braking as a control inputs, scheduled by the car velocity and by the driver performance estimation.

The paper is organized as follows. Section 2 presents the velocity dependent LPV driver model. Section 3 explains the LPV PI Observer designed to estimate the errors made by a real driver. Section 4 introduces the control-

⋆ This work is supported by the French National Research Agency in the framework of the "Investissemnts d'avenir" program ANR-15-IDEX-02. This work has also been partially funded by the Spanish State Research Agency (AEI) and the European Regional Development Fund (ERFD) through the project SCAV (ref. MINECO DPI2017-88403-R) and by FPI UPC grant 2020FPI-UPC-008.

oriented model used for the ADAS controller synthesis. Section 5 presents the design of the LPV lateral control for ADAS. Finally, in Section 6 simulation results shows the performance of the proposed strategy in an emergency maneuver scenario. Throughout the paper all variables in red represent the scheduling variables used in the LPV formulation.

2. AN LPV DRIVER MODEL

One of the main motivations of this study is that most of Driver Models (DM) given in the literature are LTI models, which are not sufficient to globally capture the driver behaviour over a wide range of vehicle speeds. To cope with this issue, in this work, the DM used in Medero et al. (2021) is extended as an LPV model function of the vehicle longitudinal speed v_x, as shown in Fig. 1.

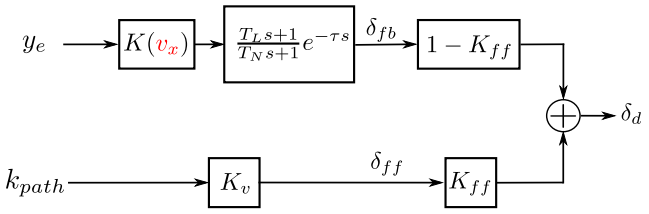

Fig. 1. LPV Driver Model

The motivation for the DM to be velocity dependent can be explained using a simple simulation, as shown in Fig. 2. The simulation scenarios, performed on a Renault Megane car model detailed in Fergani et al. (2016), are the following:

- First (in blue), an LTI DM steers a vehicle in order to perform a Double Lane Change (DLC) at a longitudinal speed of $v_x = 40m/s$. The parameters of the DM are selected to perform such maneuver with a smooth trajectory and no overshoot.
- Then (in red), the same LTI DM is used to steer the vehicle but considering a vehicle speed at $v_x = 25m/s$.

From Fig 2, it can be seen that by employing a unique LTI DM we obtain too large variations of the car trajectory when tested at different speeds, which presents to use this LTI DM as a reference model when varying vehicle speeds are considered.

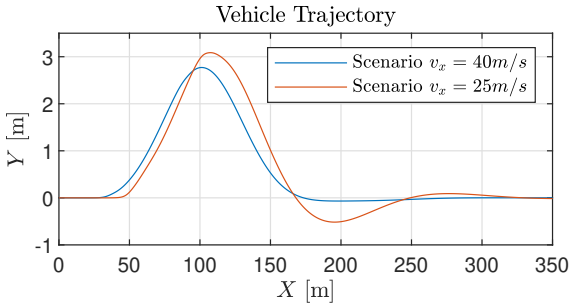

Fig. 2. Steering test of one LTI DM at different speeds

To solve this issue, the gain K in the driver model is modified to be parameter dependent, and denoted $K(v_x)$ in Fig. 1. This change allows to obtain a homogeneous trajectory of the vehicle for a wide range of speeds. The value of $K(v_x)$ is then chosen so that at all speeds the DM performs the DLC with a trajectory close to the first scenario (in blue) from Fig. 2, as detailed below:

Table 1. Values of $K(v_x)$ for Different Speeds

v_x $[m/s]$	25	30	35	40
K	1/11	1/17.5	1/21	1/26

This information can then be used to obtain a suitable value for $K(v_x)$ for any v_x within the range of 25 to 40m/s by interpolation. Notice that the values of the parameter dependent gain decrease with v_x, which makes physical sense, as it is to be expected that at higher speeds the amount of steering gain required will be smaller than at lower speeds.

From the DM presented in Fig. 1, it can be seen that the model is characterized with the set of parameters

$$\mathcal{P} = \{K(v_x), T_L, T_N, \tau, K_v, K_{ff}\} \in \mathbb{R}^6 \tag{1}$$

Let us first consider a nominal DM with parameters $P_0 \in \mathcal{P}$. Parameters P_0 are chosen as to characterize a driver with a fast reaction time, so that it can perform emergency maneuvers, as the DLC, with reduced lateral acceleration and small overshoots when compared with real drivers.

Then, this nominal DM is represented into a discrete LPV state-space model (considering a sample time $T_s = 0.01s$) as follows:

$$\begin{cases} x_d(k+1) = A_0 \cdot x_d(k) + B_0 \cdot u_d(k) \\ \delta_d(k) = C_0(v_x) \cdot x_d(k) + D_0(v_x) \cdot u_d(k) \end{cases} \tag{2}$$

with

$$u_d(k) = \begin{bmatrix} y_e(k - \tau_0/T_s) \\ k_{path}(k) \end{bmatrix} \tag{3}$$

where $x_d \in \mathbb{R}$ is the state of the DM, $u_d \in \mathbb{R}^2$ are the inputs of the driver model and $\delta_d \in \mathbb{R}$ is the steering output of the DM. Notice that the pure delay in Fig. 1, is treated in (3) as an input delay where $\tau_0 \in P_0$. Notice also that the output matrices of the DM depend on the longitudinal velocity, as these terms are function of $K(v_x)$.

Different from the nominal DM, the steering of a real driver δ_f is modelled as the following additive fault representation:

$$\delta_f(k) = \delta_d(k) + f(k) \tag{4}$$

3. DRIVER ERROR DETECTION

The objective is now to synthetize a PI observer in order to estimate f. In that framework, the fault f is assumed to be such that $\dot{f} = 0$, which could be conservative since it means that the theoretical approach is valid only for slow varying fault (even if the results will show the efficiency of the approach when f varies).

By incorporating $f(k)$ as a state variable, the extended faulty driver model is then given by:

$$\begin{cases} \begin{bmatrix} x_d(k+1) \\ f(k+1) \end{bmatrix} = \begin{bmatrix} A_0 & 0 \\ 0 & 1 \end{bmatrix} \cdot \begin{bmatrix} x_d(k) \\ f(k) \end{bmatrix} + \begin{bmatrix} B_0 \\ 0 \end{bmatrix} \cdot u_d(k) \\ \qquad\qquad + \begin{bmatrix} 1 \\ 0 \end{bmatrix} \cdot \bar{d}(k) \\ \delta_f = \begin{bmatrix} C_0(v_x) & 1 \end{bmatrix} \cdot \begin{bmatrix} x_d(k) \\ f(k) \end{bmatrix} + D_0(v_x) \cdot u_d(k) \end{cases} \tag{5}$$

where the disturbance input $\bar{d}(k) \in \mathbb{R}$ represents high-frequency uncertainties to account for unmodeled dynamics neglected in the simplified nominal DM (2).

The above driver error $f(k)$ can then be estimated with the aid of an LPV PI observer of the form:

$$\begin{cases} \begin{bmatrix} \hat{x}_d(k+1) \\ \hat{f}(k+1) \end{bmatrix} = \begin{bmatrix} A_0 & 0 \\ 0 & 1 \end{bmatrix} \cdot \begin{bmatrix} \hat{x}_d(k) \\ \hat{f}(k) \end{bmatrix} + \begin{bmatrix} B_0 \\ 0 \end{bmatrix} \cdot u_d(k) \\ \qquad\qquad -L(v_x) \cdot (\delta_f - \hat{\delta}_f) \\ \hat{\delta}_f = \begin{bmatrix} C_0(v_x) & 1 \end{bmatrix} \cdot \begin{bmatrix} \hat{x}_d(k) \\ \hat{f}(k) \end{bmatrix} + D_0(v_x) \cdot u_d(k) \end{cases} \tag{6}$$

According to (6) and with the interconnection as shown in Fig. 3, where W_D is a high-pass filter approximating the high-frequency uncertainties and W_F is a low-pass filter used to ensure the observer estimation convergence performance at low-frequencies, the extended observer error dynamics are given by:

$$\begin{cases} x_O(k+1) = A(\theta) \cdot x_O(k) + B(\theta) \cdot d(k) \\ z_e(k) = C(\theta) \cdot x_O(k) \end{cases} \tag{7}$$

with $x_O \in \mathbb{R}^{2+n_D+n_F}$ the estates of the extended error dynamics (with n_D the order of the low-pass filter W_D and n_F the order of the high-pass filter W_F), $z_e \in \mathbb{R}$ the estimation error for the additive fault f and $\theta = v_x \in \mathbb{R}$ the vector of LPV scheduling parameters.

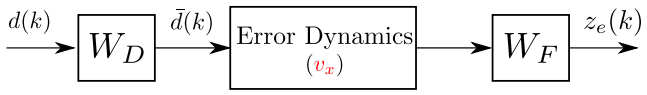

Fig. 3. PI Observer Error Dynamics Interconnection with Filters W_D and W_F

The objective for observer gain synthesis is then to minimize the induced $\mathcal{L}_2$ norm of the LPV PI observer estimation error from disturbance d to observer estimation error z_e.

$$\|z_e\|_2 \leq \gamma_\infty \|d\|_2 \tag{8}$$

The synthesis of the LPV / $\mathcal{H}_\infty$ observer gain consists in applying the Bounded Real Lemma (BRL) to the extended observer error dynamics (7). When considering a Parameter Dependent Lyapunov Matrix, such a solution is defined by an infinite set of Linear Matrix Inequalities (due to the infinite number of parameter values). To reduce it to a finite dimensional problem, the referred-to-as grid based approach is here used. It is well known for the case of continuous-time systems Wu (1995) by incorporating the parameter derivatives into the LMI formulation. In this work, considering discrete-time PDLM, it is used a discrete version of the parameter derivatives approach by considering increments on the parameter variations. A similar approach can be found in Na and Ke-You (2007).

The existence of the observer gain $L(\theta)$ is given in the following theorem.

Theorem 1. Given the discrete-time observer error extended dynamics (7), gridded at N grid points for M varying parameters, the parameter dependent observer gain $L(\theta)$ exists if there exists a PDLM $X(\theta) \in \mathbb{R}^{2+n_F+n_D}$, $X(\theta) = X(\theta)^T > 0$ such that the following LMI optimization problem is feasible:

$$\min \lambda \ \text{ s.t.}$$
$$X(\theta_i) > 0, \ X(\theta_i^j) > 0 \tag{9}$$

$$\mathcal{N}_{Pi}^T \begin{pmatrix} A_i^T X(\theta_i^j) A_i - X(\theta_i) & A_i^T X(\theta_i^j) B_i & C_i^T \\ * & B_i^T X(\theta_i^j) B_i - \lambda I & 0 \\ * & * & -I \end{pmatrix} \mathcal{N}_{Pi} \leq 0 \tag{10}$$

$$\forall (i = 1, 2, ..., N; j = 1, 2, ..., 2^M) \text{ combinations}$$

with

$$\mathcal{N}_{Pi} = \text{null} \left(\begin{bmatrix} \begin{bmatrix} C_{0i} & 1 \end{bmatrix} & 0 & 0 \\ 0 & 0 & 0 \\ 0 & 0 & 0 \end{bmatrix}, \ 0, \ 0 \right) \tag{11}$$

where the sub index i indicates that the element has been frozen at the i grid point of the LPV system, and for each frozen grid point i, then the upper index j corresponds to a vertex of the bounding box for $\theta_i(k+1)$. Then, the upper bound of the induced $\mathcal{L}_2$ norm of the LPV system is given by $\gamma_\infty = \sqrt{\lambda}$.

Sketch-of-Proof: This theorem is the dual version of the more standard control problem solution, presented later in Theorem 2. ■

If there exists a feasible PDLM $X(\theta)$, the parameter dependent observer gain $L(\theta) \in \mathbb{R}^2$ can then be computed over the BRL LMI applied to the extended error dynamics (7). This two steps approach is identical as introduced in Gahinet and Apkarian (1994), with the difference that the LMIs are applied here at each frozen grid point.

For the driver error detection PI Observer, the shaping filters have been considered of order $n_D = 2$ and $n_F = 6$. The chosen PDLM is as:

$$X(v_x) = X_0 + \frac{1}{v_x} X_1 + \frac{1}{{v_x}^2} X_2 \tag{12}$$

with considered grid points:

$$v_{xi} = [25, 27.5, 30, 32.5, 35, 37.5, 40] \tag{13}$$

and maximum parameter variation rate $\Omega = 3$.

4. INTEGRATED DRIVER-VEHICLE CONTROL ORIENTED MODEL

To tackle the design of the ADAS controller, the control-oriented model cannot be the lateral dynamics of the vehicle alone, as the steering applied by the driver is of critical importance to the stability of the overall system. So the driver must be taken into account.

To incorporate the driver in the control loop, the nominal DM (2) is considered. As in Medero et al. (2021), for control design, the DM is modified by considering the relationship:

$$k_{path} = \frac{\dot{\psi}_{ref}}{v_x} \tag{14}$$

This results in the inputs to the DM modified as:

$$u_d = \begin{bmatrix} y_e & \dot{\psi}_{ref} \end{bmatrix}^T, \tag{15}$$

and in the feedforward gain given as K_v / v_x.

On the other hand, for modelling the lateral dynamics of the vehicle it is used the well-known bicycle model with steering angle and generated yaw moment as control inputs.

$$\begin{bmatrix} \ddot{y} \\ \ddot{\psi} \end{bmatrix} = \begin{bmatrix} -\frac{C_{\alpha f}+C_{\alpha r}}{m v_x} & -v_x - \frac{C_{\alpha f} l_f - C_{\alpha r} l_r}{m v_x} \\ -\frac{C_{\alpha f} l_f - C_{\alpha r} l_r}{I_z v_x} & -\frac{C_{\alpha f} l_f^2 + C_{\alpha r} l_r^2}{I_z v_x} \end{bmatrix} \begin{bmatrix} \dot{y} \\ \dot{\psi} \end{bmatrix} + \begin{bmatrix} \frac{C_{\alpha f}}{m} & 0 \\ \frac{C_{\alpha f} l_f}{I_z} & \frac{1}{I_z} \end{bmatrix} \begin{bmatrix} \delta \\ M_z \end{bmatrix} \tag{16}$$

The generated yaw moment M_z is produced by means of differential braking, with braking torques T_{brl} and T_{brr} for the left and right rear wheels respectively, computed according to the following relations:

$$T_{brl} = \begin{cases} \frac{R \cdot M_z}{t_f}, & \text{if } M_z \geq 0 \\ 0, & \text{otherwise} \end{cases}, \; T_{brr} = \begin{cases} \frac{-R \cdot M_z}{t_f}, & \text{if } M_z < 0 \\ 0, & \text{otherwise} \end{cases} \tag{17}$$

R is the radius of the wheel and t_f is the distance from the wheel to the center-line of the car. Finally, the interconnection of the driver-vehicle open-loop system can be seen in Fig. 4

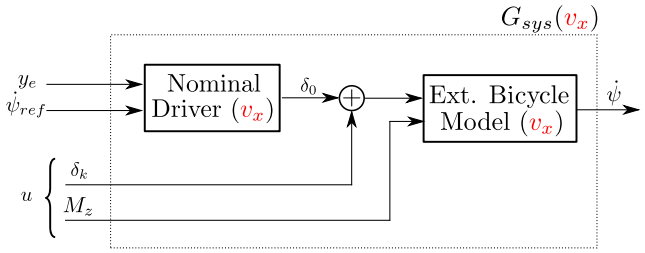

Fig. 4. Integrated Driver-Vehicle Control Model

5. ROBUST LPV ADAS STRATEGY

5.1 Integrated LPV ADAS Strategy

The proposed strategy for the ADAS system is presented in Fig. 5. In the first place, the human driver is steering the vehicle, whose real dynamics and driving ability are unknown. From the PI Observer presented in Sect. 3, we can estimate how much the real driver is moving away from the virtual nominal driver steering actions through the estimated $\hat{f}(k)$. This estimation is used as input of both scheduling functions, ρ_1 and ρ_2, modifying the behaviour of the ADAS controller. As detailed below, ρ_1 affects the magnitude of the steering command δ_k and ρ_2 the magnitude of the differential yaw moment command M_z.

The LPV ADAS controller $K(v_x, \rho_1, \rho_2)$ acts in parallel to the human driver. The objective of the scheduling signals ρ_1, ρ_2 are to penalize the ADAS controller commands in nominal situations while allowing greater control authority in the case of poor driver performance.

Notice the presence in the scheme of external signals y_e, k_{path} and $\dot{\psi}_{ref}$. In the proposed ADAS strategy, these signals are supposed to be generated by some planner at the high-level guidance stage, which is outside the scope of this paper.

5.2 Fault Dependent Scheduling Functions

As in Medero et al. (2021), the estimation fault is not directly used, but the relative fault instead:

$$\bar{f}(k) = \frac{\hat{f}(k)}{f_0}, \tag{18}$$

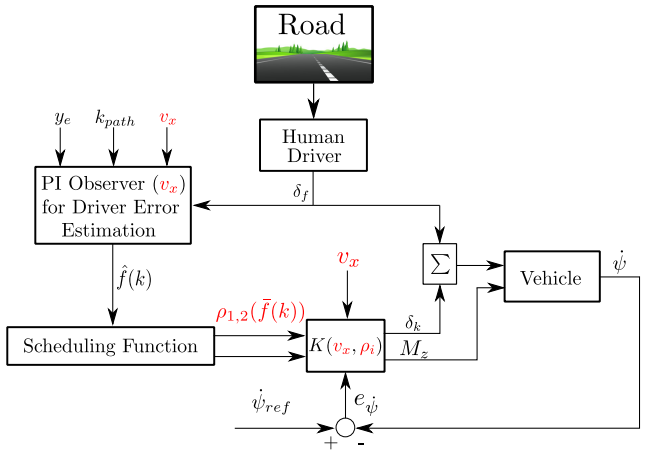

Fig. 5. Combined Driver Error Detection / ADAS Controller Scheme

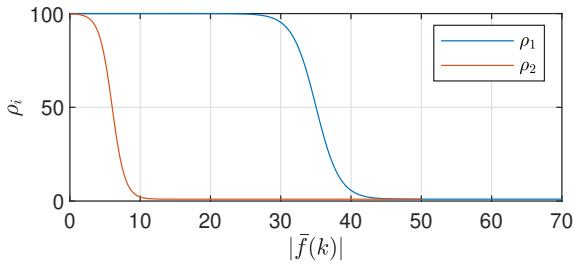

Fig. 6. Driver Error Based Scheduling Functions

where f_0 is a threshold value defining the maximum additive fault estimation not considered as an actual fault.

The scheduling functions $\rho_i(\bar{f}(k))$, $i = 1, 2$, shapes are given in 6. These shapes have been selected so that for low / medium levels of $|\bar{f}(k)|$, the function ρ_2 will drop to zero. Meanwhile the function ρ_1 will drop only when very large values of driver error are being estimated, corresponding to more dangerous situations. The effect of this choice is that the use of yaw moment command M_z would be given priority over the steering command δ_k, which is reserved for critical scenarios only. Note that it is desired not to interfere with the driver steering unless it is ultimately required.

5.3 LPV / $\mathcal{H}_\infty$ ADAS Controller

The control problem is here formulated as an LPV / $\mathcal{H}_\infty$ problem where the objective is to minimize the induced $\mathcal{L}_2$ norm of the LPV closed-loop from exogenous inputs w to exogenous outputs z:

$$\|z\|_2 \leq \gamma_\infty \|w\|_2 \tag{19}$$

More specifically, the general plant P for the induced $\mathcal{L}_2$ norm problem including the State-Feedback ADAS controller is given in Fig. 7.

Note that performance weights are included to tackle the different objectives. The weight W_e is a first-order transfer function used for regulation purposes, with the yaw rate error $e_{\dot{\psi}}$ as input. To shape the response of the control actions, each of the control inputs is weighted by a LPV bandpass filter $W_{u_i}(\rho_i)$, $i = 1, 2$:

$$W_{u_i}(\rho_i) = \rho_i W_{u_i} \tag{20}$$

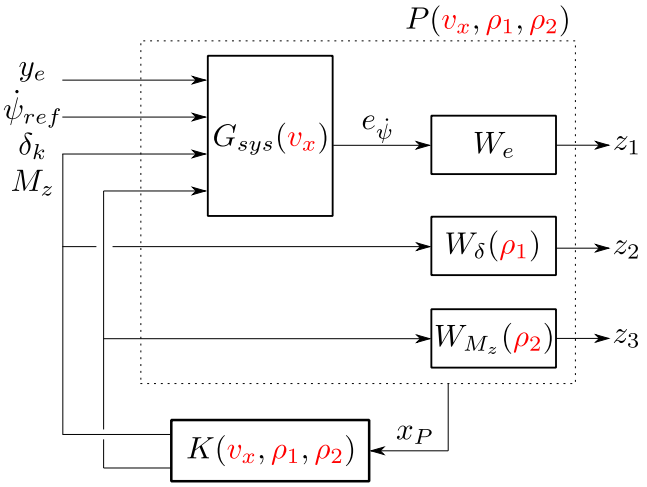

Fig. 7. LPV / $\mathcal{H}_\infty$ Generalized Plant P for the State-Feedback Problem

with W_{u_i} as in Doumiati et al. (2013). The objectives of this filter is to constrain the controller actuator i to act in a narrow frequency range. Concerning the additional steering command δ_k, the weight W_δ is constrained to the frequencies $f_a = 1$ and $f_b = 10$ Hz. In this range, the additional steering can affect the dynamics of the vehicle without being felt invasive to the driver, who is mainly sensitive to steady-state frequencies ($\leq$ 1Hz) and high frequencies ($\geq$ 10Hz) affecting the steering wheel. Also, in the spirit of reduced interference, the maximum gain of the filter has been selected to bound the additive steering command δ_k to the range [-2,2] degrees. Meanwhile, the weight W_{M_z} is bounded by the frequencies $f_a = 1$ and $f_b = 50$ Hz, where f_b is the bandwidth of the brakes and f_a, as before, has been selected to avoid constant control actions that would feel intrusive to the driver.

Notice that control performance weights change according to the scheduling signals ρ_i. Therefore, when the scheduling functions are at their maximum value they penalize the corresponding control action, meanwhile when they are at the lowest values, the corresponding control command is given control authority. This achieves the interconnection between driver error estimation and controller activation / deactivation in an LPV manner.

5.4 LPV / $\mathcal{H}_\infty$ State-Feedback Synthesis

From the discretized nominal DM/lateral dynamics model with performance weights, Fig. 7, define the open-loop generalized plant P as:

$$\begin{cases} x_P(k+1) = A(\theta) \cdot x_P(k) + B_u(\theta) \cdot u(k) + B_w(\theta) \cdot w(k) \\ z(k) = C(\theta) \cdot x_P(k) + D_u(\theta) \cdot u(k) + D_w(\theta) \cdot w(k) \end{cases} \tag{21}$$

where $x_P \in \mathbb{R}^8$ are the states of P, $u \in \mathbb{R}^2$ are the control inputs, $w \in \mathbb{R}^2$ are the exogenous inputs and $z \in \mathbb{R}^3$ are the exogenous outputs.

The synthesis of the LPV / $\mathcal{H}_\infty$ State-Feedback controller consists in applying the Bounded Real Lemma (BRL) over (21). In order to reduce such a problem to a finite dimension the grid based approach is used. Considering a PDLM $X(\theta(k))$, with the vectors of varying parameters defined as $\theta(k) = [v_x(k), \rho_1(k), \rho_2(k)] \in \mathbb{R}^3$. The existence of the Parameter Dependent LPV State-Feedback controller $K(\theta)$ is given in the following theorem.

Theorem 2. Given a discrete-time open-loop LPV System (21), gridded at N grid points for M varying parameters, the State-Feedback controller $K(\theta)$ exists if there exists a PDLM $X(\theta) \in \mathbb{R}^8$, $X(\theta) = X(\theta)^T > 0$ such that the following LMI optimization problem is feasible:

$$\min \lambda \ \text{ s.t.}$$
$$X(\theta_i) > 0, \ X(\theta_i^j) > 0 \tag{22}$$

$$\mathcal{N}_{Wi}^T \begin{pmatrix} A_i X(\theta_i^j) A_i^T - X(\theta_i) & A_i X(\theta_i^j) C_i & B_{wi} \\ * & C_i X(\theta_i^j) C_i - \lambda I & D_{wi} \\ * & * & -I \end{pmatrix} \mathcal{N}_{Wi} \leq 0 \tag{23}$$

$$\forall (i = 1, 2, ..., N; j = 1, 2, ..., 2^M) \text{ combinations}$$

with

$$\mathcal{N}_{Wi} = \text{null}\left([B_{ui}^T, D_{ui}^T, 0]\right) \tag{24}$$

where the sub index i indicates that the element has been frozen at the i grid point of the LPV system, and for each frozen grid point i, then the upper index j corresponds to a vertex of the bounding box for $\theta_i(k+1)$. Then, the upper bound of the induced $\mathcal{L}_2$ norm of the LPV system is given by $\gamma_\infty = \sqrt{\lambda}$.

Sketch-of-Proof: Theorem 2 is based on standard results for the discrete-time $\mathcal{H}_\infty$ control synthesis based on LMIs, as presented by Gahinet and Apkarian (1994). It is here extended to the LPV PDLM $X(\theta(k))$ case and applied to the State-Feedback problem.

Note that, in the BRL LMI of the Parameter Dependent Lyapunov function approach for discrete-time systems, both $X(\theta(k))$ and $X(\theta(k+1))$ do appear. If a grid-based approach is considered, then for a frozen value θ_i of the parameter grid, the PDLM can be evaluated as $X(\theta_i)$. Then, if the maximum variation rate Ω of the varying parameter is known, the varying parameter can be bounded as follows:

$$\theta_i(k+1) \in [\theta_i - T_s \cdot \Omega, \ \theta_i + T_s \cdot \Omega], \tag{25}$$

The PDLM $X(\theta(k+1))$ evaluated at each vertex due to parameter bounding is here written as $X(\theta_i^j)$.

Following this approach, the BRL applied to closed-loop interconnection does not lead to an LMI due to multiplication of $X(\theta)$ and $K(\theta)$. However, applying the Projection Lemma the controller block can be eliminated. Followed by a Schur Lemma over $-X(\theta_i^j)^{-1}$, the LMI conditions (22)-(23) are recovered. ■

If there exists a feasible PDLM $X(\theta)$, the parameter dependent state-feedback controller $u(k) = K(\theta) \cdot x_P(k)$ can then be computed using the BRL LMI over the closed-loop interconnection of (21).

The considered PDLM $X(\theta(k))$ for the ADAS controller problem is chosen as:

$$X(\theta(k)) = X_0 + v_x X_1 + \frac{1}{v_x} X_2 + \rho_1 X_3 + \rho_2 X_4 \tag{26}$$

With considered grid points for each varying parameter:

$$v_{xi} = [25, 27.5, 30, 32.5, 35, 37.5, 40] \tag{27}$$
$$\rho_{1i} = [1, 10, 100] \tag{28}$$

$$\rho_{2i} = [1, 10, 100] \tag{29}$$

And the vector of maximum variation rates of the parameters as $\Omega = [3, 600, 600]$.

6. RESULTS

To test the performance of the proposed lateral ADAS control some simulations have been performed. The considered vehicle is a full car model of a Renault Megane presented in Fergani et al. (2016). The parameters of the nominal DM, used both for controller synthesis and the driver-error estimator PI Observer, can be found in Tab. 2. Two simulation scenarios are tested:

- In the first scenario the driver must perform a DLC emergency maneuver without ADAS assistance.
- In the second scenario the same driver must perform the same maneuver, this time with ADAS assistance.

For both scenarios, ten randomly generated drivers profiles have been considered. To simulate a real driver, the parameters of these randomized DM are values close to a real human. The range in which the randomized faulty parameters can lie are given in Tab. 2. The profile of the longitudinal speed v_x the vehicle experience is shown in Fig. 8.

Table 2. DM Parameters

Parameter	Nominal	Faulty Range
T_L	0.3	[0.2, 0.3]
T_N	0.1	[0.14, 0.25]
τ	0.1	[0.15, 0.22]
K_v	1.4	[1.1, 1.5]
K_{ff}	0.85	[0.75, 0.85]

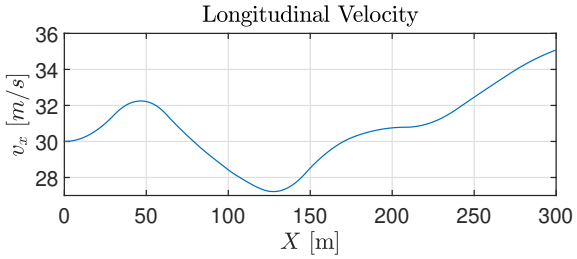

Fig. 8. Longitudinal Speed Profile of the Vehicle During Simulations

The simulation results for both scenarios are shown in Fig. 9. In this figure it can be seen at the top, data from the scenario without assistance, with the vehicle trajectory at the top-left and the vehicle lateral acceleration at the top-right. At the bottom, data for the case when ADAS assistance is active are shown, the vehicle trajectory at the bottom-left and the vehicle lateral acceleration at the top-right.

From the data it can be seen that in the case without ADAS, the performances of the generated drivers are very different. Some have very poor performances, which in a real scenario would lead to an accident if such maneuver is carried, while others can accomplish the DLC in a safer manner, although some oscillations are still present in their trajectory. In the scenario where the ADAS controller is used, it can be seen that the performances are quite homogeneous in between all ten drivers, both in terms of the vehicle trajectory and lateral acceleration. When the proposed ADAS is used, the trajectories during the DLC can be seen to be smoother, and once finished the DLC, the oscillations in the trajectories are greatly reduced. Moreover, in the scenario with ADAS, the lateral acceleration the vehicle experiences are less than half the ones of the case without ADAS. This is significant as high values of lateral acceleration at high-speeds can cause the vehicle to oversteer.

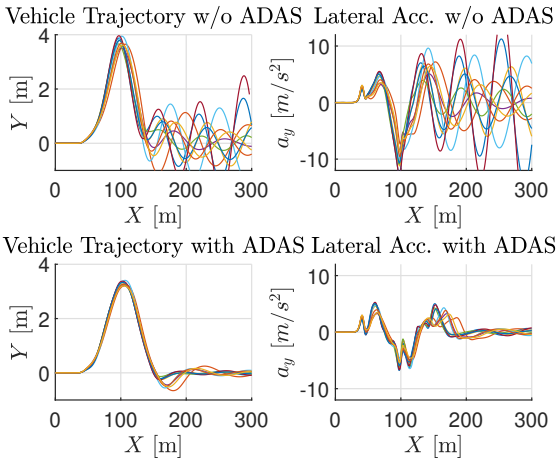

Fig. 9. Driving Comparison with and w/o ADAS During DLC Maneuver

Information regarding the controller scheduling and controller commands for the second scenario can be found in Fig. 10 and Fig. 11. For the sake of clarity of presentation, each figure represents data from a single driver, Fig. 10 and Fig. 11 corresponding to the worst and best performers respectively out of the ten generated drivers. In both figures it is shown in top the scheduling signals used to modulate the magnitude of the controller actions, it is shown in the top-left ρ_1 (affects the additive steering command) and at the top-right ρ_2 (affects the differential torque M_z command). On the bottom, it is shown the control inputs themselves, on the bottom-left the steering command δ_k and on the bottom-right the braking torque command for the left (T_{brl}) and right (T_{brr}) rear wheels.

For the worst case driver, Fig 10, it can be seen that an important driver error is being estimated, as both scheduling functions reach low values. Therefore, the LPV reconfiguration needs to activate the additive steering control input to assist the driver successfully. For the best driver in Fig. 11, however, the magnitude of driver error estimated is less, and then the commanded braking torques are half in magnitude than those of the previous case. It is worth noting that in this case the steering command is not activated, as it is desired to be only used for the most critical scenarios.

7. CONCLUSION

In this study, a lateral control strategy for ADAS has been presented. The main contributions of the strategy are the detection of drivers performances with the use of an LPV PI Observer and the employment of these estimations of driver's performances to schedule the LPV lateral vehicle

controller. As seen in the simulation results, the proposed LPV driver error estimation / ADAS controller strategy achieves the paper's objective: to minimize the ADAS intrusiveness in the driver experience without compromising on safety when required, all while being robust to a broad range of driver behaviours and changes in vehicle velocity.

Future studies will concern testing the strategy in more realistic simulation scenarios and possibly in simulators with real human drivers. Additionally it will be considered the usage of more sophisticated scheduling strategies for the LPV lateral vehicle controller based on learning approaches rather than the hyperbolic functions used in this work.

REFERENCES

Chen, Y., Zhang, X., and Wang, J. (2019). Robust vehicle driver assistance control for handover scenarios considering driving performances. *IEEE Transactions on Systems, Man, and Cybernetics: Systems*.

Doumiati, M., Sename, O., Dugard, L., Martinez-Molina, J.J., Gaspar, P., and Szabo, Z. (2013). Integrated vehicle dynamics control via coordination of active front steering and rear braking. *European Journal of Control*, 19(2), 121–143. doi: https://doi.org/10.1016/j.ejcon.2013.03.004.

Erlien, S.M., Fujita, S., and Gerdes, J.C. (2015). Shared steering control using safe envelopes for obstacle avoidance and vehicle stability. *IEEE Transactions on Intelligent Transportation Systems*, 17(2), 441–451.

Fergani, S., Sename, O., and Dugard, L. (2016). An lpv/$\mathcal{H}_\infty$ integrated vehicle dynamic controller. *IEEE Transactions on Vehicular Technology*, 65(4), 1880–1889. doi:10.1109/TVT.2015.2425299.

Gahinet, P. and Apkarian, P. (1994). A linear matrix inequality approach to $\mathcal{H}_\infty$ control. *International journal of robust and nonlinear control*, 4(4), 421–448.

Gáspár, P., Németh, B., and Bokor, J. (2012). Design of integrated vehicle control using driver models. *IFAC Proceedings Volumes*, 45(13), 517–522.

Guzman, J., López-Estrada, F.R., Estrada-Manzo, V., and Valencia-Palomo, G. (2021). Actuator fault estimation based on a proportional-integral observer with non-quadratic lyapunov functions. *International Journal of Systems Science*, 1–14.

Ji, X., Yang, K., Na, X., Lv, C., and Liu, Y. (2018). Shared steering torque control for lane change assistance: a stochastic game-theoretic approach. *IEEE Transactions on Industrial Electronics*, 66(4), 3093–3105.

Khosravani, S., Khajepour, A., Fidan, B., Chen, S.K., and Litkouhi, B. (2014). Development of a robust vehicle control with driver in the loop. In *2014 American Control Conference*, 3482–3487. IEEE.

Mars, F., Deroo, M., and Hoc, J.M. (2014). Analysis of human-machine cooperation when driving with different degrees of haptic shared control. *IEEE transactions on haptics*, 7(3), 324–333.

Medero, A., Sename, O., and Puig, V. (2021). Control reconfiguration of lateral adas steering control in the presence of driver errors using combined parity space / lpv approaches. In *2021 5th International Conference on Control and Fault-Tolerant Systems (SysTol)*, 7–12. doi:10.1109/SysTol52990.2021.9595648.

Na, W. and Ke-You, Z. (2007). Parameter-dependent lyapunov function approach to stability analysis for discrete-time lpv systems. In *2007 IEEE International Conference on Automation and Logistics*, 724–728. doi: 10.1109/ICAL.2007.4338659.

Saleh, L., Chevrel, P., Claveau, F., Lafay, J.F., and Mars, F. (2013). Shared steering control between a driver and an automation: Stability in the presence of driver behavior uncertainty. *IEEE Transactions on Intelligent Transportation Systems*, 14(2), 974–983.

Wu, F. (1995). *Control of linear parameter varying systems*. Ph.D. thesis, University of California, Berkeley.

Youssef, T., Chadli, M., Karimi, H.R., and Wang, R. (2017). Actuator and sensor faults estimation based on proportional integral observer for ts fuzzy model. *Journal of the Franklin Institute*, 354(6), 2524–2542.

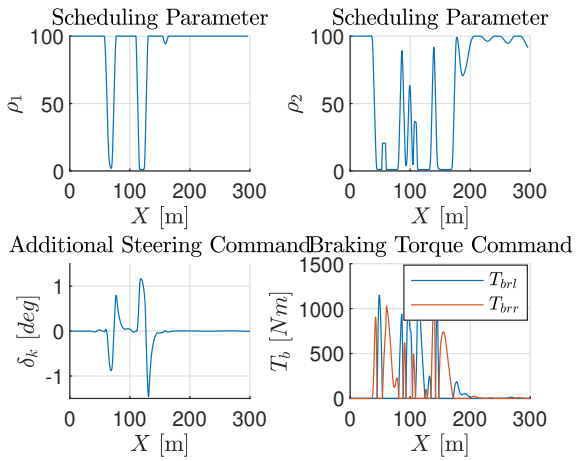

Fig. 10. Scheduling Signals and Actuator's Commands for the Case of Worst Driver Performance

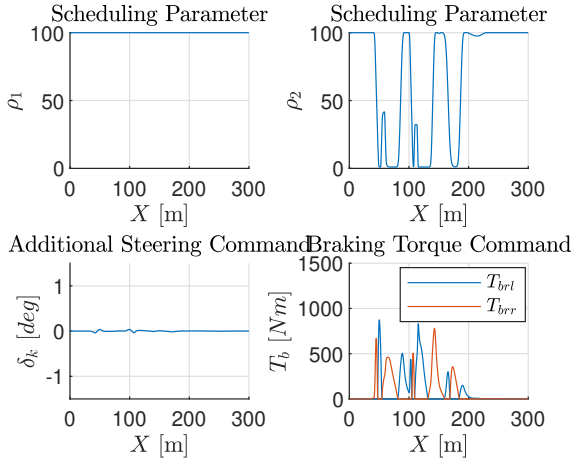

Fig. 11. Scheduling Signals and Actuator's Commands for the Case of Best Driver Performance